

# Brittle Failure and Crack Initiation Angle in Plates Weakened by V- and U-Notches Under Mixed Mode (I+II) Loading

F. Berto<sup>1</sup>, P. Lazzarin<sup>1</sup>, M. Elices<sup>2</sup>, F.J. Gómez<sup>2</sup>

<sup>1</sup> Department of Management and Engineering, University of Padova, Stradella S.Nicola 3, 36100, Vicenza (Italy)

<sup>2</sup> Department of Materials Science – Universidad Politécnica de Madrid E.T.S. Ingenieros de Caminos – 28040 Madrid (Spain)

**ABSTRACT.** *The paper presents a large bulk of experimental data from U- and V-notched beams under mixed mode loading. The reanalysis concern data from specimens made of PMMA tested by the authors at -60°C as well as other data taken from the recent literature. The synthesis is carried out by using the mean value of the strain energy density (SED) over a given control volume.*

*Afterwards the problem of the crack initiation angle for U-notches is analysed on the basis of the maximum principal stress located on the notch edge, outside the notch bisector line. Finally, dealing with cracked and very sharp V-notches subjected to mixed mode (I+II), predictions based on the maximum tangential stress or the minimum strain energy density criteria are compared. The influence of the singular and non-singular stress terms on the crack initiation angle is discussed.*

## INTRODUCTION

In the last years different criteria were proposed to assess brittle or quasi-brittle failures under monotonic loading [1-5]. The problem has been extensively analysed also by the present authors by means of theoretical, numerical and experimental analyses based on the Cohesive Zone Model [4] and the Strain Energy Density (SED) concept [3, 5]. Both methods were used to summarise data of static failures from sharp and blunt notches under mode I and mixed mode (I+II) loading [6-8].

The local SED was determined on the same finite volume already defined for Mode I loading, but rigidly rotated along the notch edge and centred with respect to the point where the elastic principal stress and the SED present their maximum value [6]. With the aim to analyse different mode I+II mixities, a large number of data from specimens weakened by tilted U-notches were considered [7]. All specimens made of PMMA were tested at -60°C to assure an ideally linear elastic behaviour. Recently the database related to PMMA tested under different mode mixity conditions was extended to a number of tilted pointed V-notches with different opening angles [8]. Those data together with new data from mixed mode, I+II, as reported by Chen and Ozaki [9] and by Ayatollahi and Aliha [10] are considered in this work focusing the attention on the

crack initiation angle at failure. Chen and Ozaki [9] tested V-notched specimens made of an acrylic resin whereas Ayatollahi and Aliha [10] proposed a new test configuration for mixed mode fracture and provided a complete set of experimental data from diagonally loaded square cracked plate specimens made of PMMA.

The main aim of the first part of the present paper is to present a complete synthesis based on the local SED in order to discuss the capability of the volume-based strain energy density approach to summarise data obtained under a large range of loading conditions and very different geometrical parameters (notch radius, opening angle, notch depth). Regardless of the mode mixity, the SED-based synthesis will result to be satisfactory also in cases very close to pure mode II loading.

The second part of the paper deals with the analysis of fracture initiation direction and early propagation. Very different fracture angles are documented, strongly dependent on the mode I and mode II stress fields ahead of the notches. The angles are summarised both for sharp and rounded notches. Dealing with sharp notches, two well-known criteria [11-12], the former due to Erdogan and Sih (1963), the latter due to Sih (1974), are used to assess the initiation angle and to compare theoretical values and experimental results. Particular attention is paid to show the influence on the fracture angles of the non-singular stress term and the distance from the notch tip.

## EXPERIMENTAL PROGRAM: PMMA TESTED AT LOW TEMPERATURE

The material chosen for the experimental programme was polymethyl-methacrylate (PMMA) tested at  $-60^{\circ}\text{C}$ , an amorphous glassy polymer that exhibits a non-linear behaviour at room temperature and linear elastic up to fracture at  $-60^{\circ}\text{C}$ , even when tested without cracks or notches. The experimental programme was performed both with U- and V-notched specimens, varying the notch inclination, the notch angle and the boundary conditions. The geometry of the specimens is shown in Fig.1. In all specimens, the thickness,  $B$ , was 14 mm, the depth,  $W$ , was 28 mm, and the notch length,  $a$ , was 14 mm.

Dealing with sharp notches [8], the notch root radius,  $R$ , was always less than 0.1 mm, ranging between 20  $\mu\text{m}$  and 72  $\mu\text{m}$ . To achieve different mixed mode loadings, two types of V-notched specimens were studied; beams with *vertical* notches, with notch angles,  $30^{\circ}$ ,  $60^{\circ}$  and  $90^{\circ}$  (Fig. 1a), and beams with *tilted* notches at  $45^{\circ}$ , with notch angles  $30^{\circ}$  and  $60^{\circ}$  (Fig. 1b) and  $90^{\circ}$  (Fig. 1c). Samples were loaded as shown in Fig. 1. When loading beams with vertical notches, the position of the loading point was modified; the distance from this point to the middle point,  $b$ , was 1 mm or 9 mm. When loading beams with tilted notches, the position of the support was moved and the horizontal distance to the centre of the specimen,  $m$ , was 9 mm or 18 mm. Notch angles higher than  $90^{\circ}$  were not considered in this research.

Dealing with U-notches [6, 7] two different geometries were tested, as indicated in Fig. 1; standard U-notched beams (Fig. 1d) and beams with a tilted U-notch (Fig. 1e), to explore a larger range of mixed modes. For vertical U-notched beams (Fig. 1d), notches with six different notch root radii,  $R$ , were tested;  $R = 0, 0.2, 0.3, 0.5, 1.0, 2.0$  and  $4.0$

mm. Mixed mode loading was achieved by changing the loading position  $b_1$ . Six values were used;  $b_1 = -3, +3, 9, 18, 27$  and  $36$  mm. All in all, 36 different samples were tested. Because each one was repeated three times, a total number of 108 tests were performed for this geometry. For tilted U-notched beams (Fig. 1e), five different notch root radii were explored;  $R = 0.3, 0.5, 1.0, 2.0$  and  $4.0$  mm. Mixed mode loading was controlled by changing the support span  $m$ , as shown in Fig. 1e. Three values of  $m$  were considered;  $m = 3, m=9$  and  $m=15$  mm.

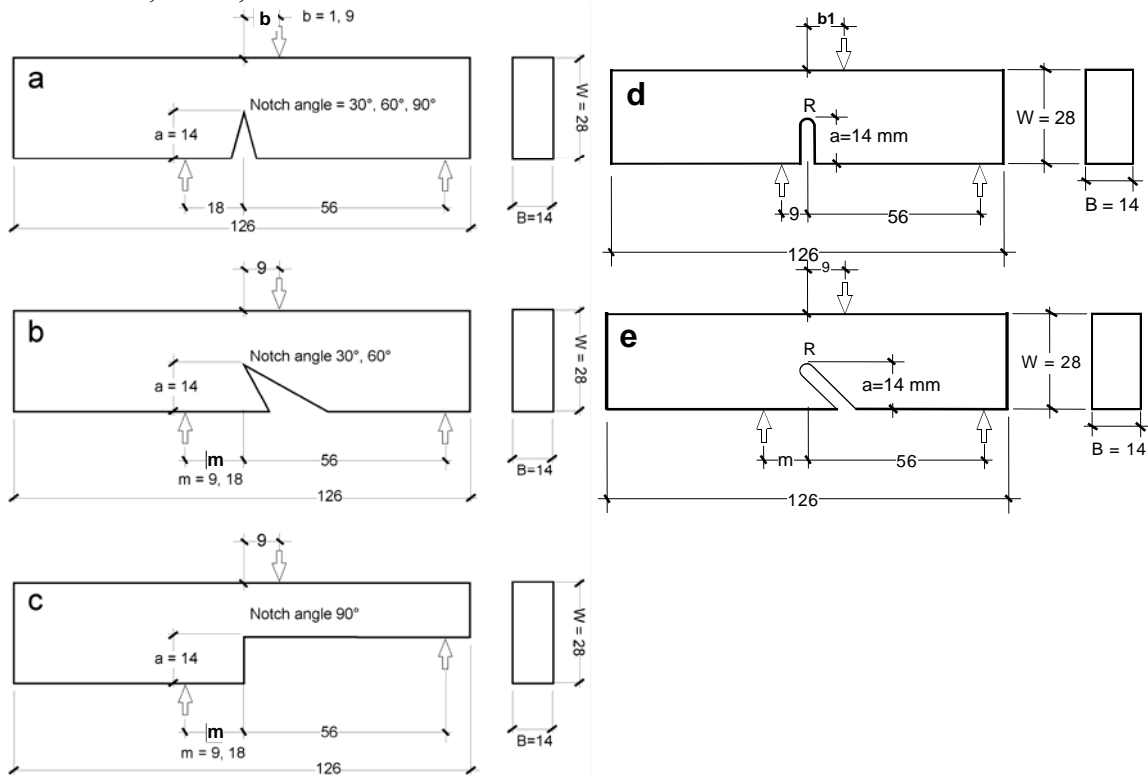


Figure 1. Geometry and loading conditions for sharp and blunt V- and U-notches [6-8].

## SYNTHESIS BASED ON STRAIN ENERGY DENSITY

A synthesis based on the strain energy over a control volume is presented in Figure 2. The data related to the experimental program of PMMA tested at  $-60^{\circ}\text{C}$  are summarised together with other data taken from a data base due to Gomez and Elices and related to PMMA tested at room temperature. Dealing with cracked and V-sharp specimens under mixed mode I+II loading recent data taken from the literature are also considered in the present synthesis [9, 10]. In particular Chen and Ozaki's data are from sharp V-specimens made of an acrylic resin and tested under mixed mode loading whereas Ayatollahi and Aliha's data [10] are from diagonally loaded square cracked plate specimens made of PMMA. The local SED values are normalised to the critical SED values (as determined from unnotched, plain specimens) and plotted as a function of the  $R/R_0$  ratio. A scatterband is obtained whose mean value does not depend on  $R/R_0$ ,

whereas the ratio between the upper and the lower limits are found to be about equal to  $1.3/0.8=1.6$  (Fig. 2). The strong variability of the non-dimensional radius  $R/R_0$  (notch root radius to control volume radius ratio, ranging here from about zero to about 500) makes stringent the check of the approach based on the local SED. The same scatterband was recently obtained by summarising failure data from 20 different ceramics, 4 PVC foams and some metallic materials [13].

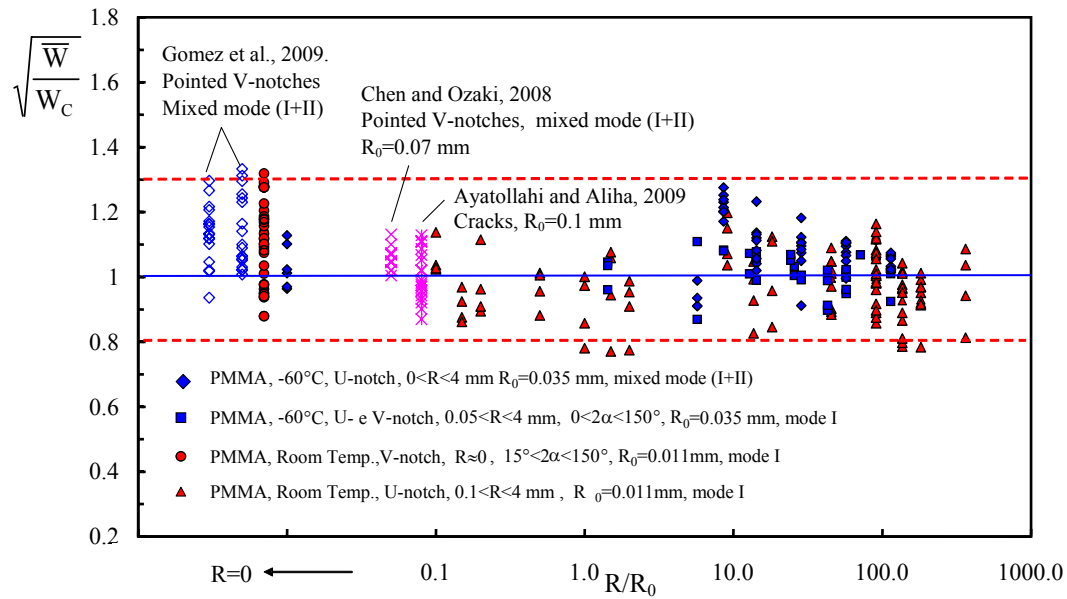


Figure 2. Static failure data in terms of normalised strain energy density

### FRACTURE INITIATION ANGLE FOR BLUNT NOTCHES

Dealing with PMMA specimens weakened by U-notches, the values of the initial crack angle,  $\varphi$ , at the notch tip (see Fig. 3) are recorded in Table 1, together with their mean value  $\langle\varphi\rangle$ . For the sake of brevity only the data referred to inclined notches are summarised in the table (see Refs [6, 7] for more details).

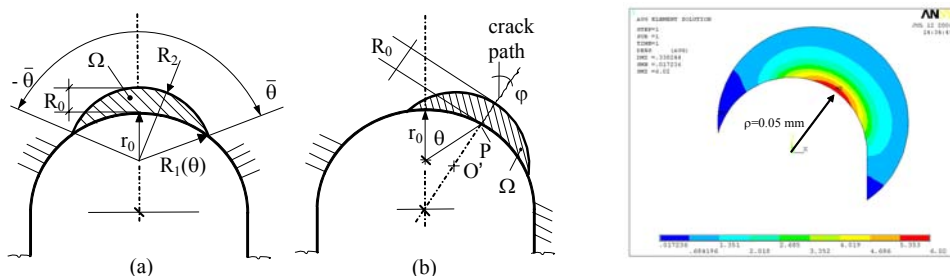


Figure 3. Control volume under mode I and mixed mode loading. Angle  $\varphi$  gives the fracture direction, evaluated experimentally in the vicinity of the notch edge.

The experimental values of crack angles (measured from the notch bisector line) are compared with the values obtained from FE analyses in correspondence of the maximum stress determined on the edge of the notch (Figure 3). The agreement is satisfactory for  $R \leq 1$  mm and  $m \geq 9$  mm whereas the difference of about  $10^\circ$  or more with  $R \leq 0.5$  mm and  $m=3$  mm.

Table 1. Comparison between experimental and numerical initial crack angles

R [mm]	m [mm]	$\varphi_1$	$\varphi_2$ [degrees]	$\varphi_3$	$\langle\varphi\rangle$ [degrees]	$\varphi$ [degrees]
			Exp.		Exp.	FEM
4	15	64.1	64.8	63.9	64.3	65.5
	9	67.2	66.6	68.7	67.5	69.5
	3	77.8	78.5	76.6	77.6	77.5
2	15	66.4	64.9	66.5	65.9	65.5
	9	67.5	68.5	76.7	70.9	68.5
	3	84.5	85.9	83.6	84.7	76.5
1	15	63.7	63.1	61.8	62.8	59.5
	9	69.3	65.9	69.2	68.1	66.5
	3	77.2	84.3	80.3	80.6	75.5
0.5	15	64.5	64.1	63.7	64.1	56.9
	9	68.4	70.3	67.9	68.9	63.5
	3	83.3	84.8	87.5	85.2	74.5
0.3	15	60.4	62.0	60.6	61.0	51.0
	9	72.6	68.1	74.2	71.6	61.0
	3	86.2	87.0	85.5	86.2	72.0

## FRACTURE INITIATION ANGLE FOR SHARP NOTCHES

The maximum tangential stress criterion and minimum strain energy density criterion are compared in Table 2 considering pure mode II loading and both plane strain and plane stress hypotheses (Poisson's ratio  $\nu=0.3$ ). For V-notches, like for cracked plates, the crack initiation angles do not depend on the distance from the notch tip.

Table 2. Crack angle for pure mode II loading according to Erdogan-Sih and Sih criteria

$2\alpha$	Erdogan-Sih	S-Factor Pl. strain	S-factor Pl. stress
0.0	70.6	82.4	79.7
30.0	65.2	82.8	80.4
45.0	62.4	82.9	80.5
60.0	59.6	82.9	80.6
90.0	53.7	82.8	80.5

It is worth noting that minimum strain energy density criterion [11] gives approximately the same crack initiation angle, regardless of notch opening angle; conversely Erdogan-Sih's criterion [10] predicts different fracture angles, which depend on  $2\alpha$ .

Presenting data from PMMA cracked plates and pointed V-notches, all tested at  $-60^\circ\text{C}$  [8], Table 3 compares measured fracture angles and theoretical values based on Erdogan-Sih and Sih's criteria. Analysing the results of Table 3, all related to a Poisson's ratio  $\nu=0.4$ , some remarks can be drawn:

- Under mixed mode loading the minimum energy density criterion and the maximum tangential stress criterion predict almost the same fracture initiation angle for pointed V-notches and cracked plates;
- For pointed V-notches the two criteria loose the independency of the distance  $r$ , at which the fracture angle is evaluated;
- The variation of the assessed fracture angle as a function of the distance  $r$  is greater for  $2\alpha=60^\circ$  and  $2\alpha=90^\circ$  than for  $2\alpha=30^\circ$ ; in the last case the influence of the distance is very weak;
- The comparison between experimental angles and theoretical values is satisfactory for the crack case and less satisfactory for the other cases.

Table 3. Mixed mode. Comparison between experimental and theoretical initial crack angles, PMMA tested at  $-60^\circ\text{C}$  ( $\nu=0.4$ ), distance  $r$  in (mm).

$2\alpha$	$b_1$	$\varphi_1$	$\varphi_2$	$\varphi_3$	$\langle\varphi\rangle$	$\varphi$ according to Erdogan-Sih [11]						$\varphi$ according to Sih [12]						
$2\alpha$	$b_1$	$\varphi_1$	$\varphi_2$	$\varphi_3$	$\langle\varphi\rangle$	$r =$	0.035	0.05	0.1	0.2	0.3	1	0.035	0.05	0.1	0.2	0.3	1
0	-3	19.1	16.4	17.6	17.7		23.7						23.4					
0	3	31.2	25.7	25.6	27.5		32.5						32.0					
0	9	37.3	-	-	37.3		38.2						37.7					
0	18	37.5	41.5	42.2	40.4		40.3						40.0					
0	27	45.7	40.0	43.5	43.1		40.2						39.8					
0	36	36.4	35.0	46.3	39.2		40.3						39.9					
30	1	12.9	14.8	7.7	11.8		8.5	8.8	9.4	10.0	10.4	11.6	8.6	8.9	9.5	10.1	10.5	11.7
60	1	11.9	15.8	14.3	14.0		4.9	5.3	6.1	7.1	7.8	10.0	4.7	5.1	5.9	6.8	7.4	9.6
90	1	5.2	5.9	6.2	5.8		4.6	5.2	6.6	8.5	9.7	14.5	3.9	4.4	5.6	7.2	8.2	12.3
30	9	19.7	29.7	24.3	24.6		17.2	17.3	18.3	19.4	20.1	22.1	16.7	17.2	18.2	19.2	19.9	21.8
60	9	14.6	27.5	21.9	21.3		10.4	11.2	12.9	14.7	15.9	19.9	10.0	10.7	12.3	14.1	15.2	18.8
90	9	17.4	16.8	21.1	18.4		7.4	8.4	10.6	13.3	15.2	21.5	6.2	7.1	9.0	11.3	12.9	18.5
30	18	54.2	59.5	59.9	57.9		36.8	37.5	38.8	40.0	40.8	42.8	36.1	36.8	38.1	39.5	40.3	42.7
60	18	47.8	49.2	48.3	48.4		25.9	27.3	30.0	32.7	34.3	38.7	24.4	25.7	28.3	31.1	32.7	37.8
90	18	40.8	33.1	36.3	36.7		16.7	18.5	22.4	26.4	28.8	35.4	14.2	15.8	19.3	23.2	25.6	33.8
30	9	63.3	69.2	64.3	65.6		50.1	50.5	51.4	52.2	52.6	53.9	52.7	53.5	54.9	56.3	57.1	59.5
60	9	43.0	49.6	56.3	49.6		40.1	41.3	43.4	45.4	46.4	49.2	39.7	41.2	44.4	47.7	49.6	55.5
90	9	49.1	49.4	45.1	47.9		28.9	30.9	34.7	38.1	39.9	44.2	25.7	28.0	32.8	38.0	41.4	52.1

The initiation fracture angles have been evaluated considering the influence of the non-singular stress term (T-stress), as suggested for the crack case by Ayatollahi and Aliha [10]. Table 4 summarises the results only for  $2\alpha=30^\circ$  and the notches shown in Fig. 1b. The introduction of the T-stress modifies the results of Table 3 but the differences are low in the close neighbourhood of the notch tip.

Table 4. PMMA tested at  $-60^\circ\text{C}$  ( $\nu=0.4$ ). Effect of the T-stress on initial crack angle

$2\alpha$	$m$	$\varphi_1$	$\varphi_2$	$\varphi_3$	$\langle\varphi\rangle$	$\varphi$ according Erdogan-Sih [11]						$\varphi$ according to Sih [12]						
$2\alpha$	$m$	$\varphi_1$	$\varphi_2$	$\varphi_3$	$\langle\varphi\rangle$	$r =$	0.035	0.05	0.1	0.2	0.3	1	0.035	0.05	0.1	0.3	0.5	1
							T-stress = 6 MPa						T-stress = 6 MPa					
30	18	54.2	59.5	59.9	57.9		38.5	39.4	41.4	43.7	45.1	50.1	37.4	38.3	40.2	42.2	43.5	47.8
							T-stress = 8 MPa						T-stress = 8 MPa					
30	9	63.3	69.2	64.3	65.6		52.3	53.1	54.7	56.6	57.7	61.7	53.9	54.8	56.6	58.4	59.6	63.1

Table 5. Experimental and theoretical fracture angles. Data from Chen and Ozaki [9].

$2\alpha$	$\beta$	$\langle\varphi\rangle$	$\varphi$ according to Erdogan-Sih [11]							$\varphi$ according to Sih [12], S-factor						
			$r =$	0.07	0.1	0.2	0.3	0.5	1	0.07	0.1	0.2	0.3	0.5	1	
30	5	6.1		5.1	5.2	5.6	5.8	6.1	6.5	5.3	5.5	5.8	6.1	6.4	6.7	
30	15	16.8		15.8	16.3	17.3	17.9	18.6	19.7	15.9	16.4	17.3	17.9	18.6	19.6	
30	30	30.0		30.6	31.2	32.6	33.4	34.4	35.7	29.1	29.7	30.8	31.5	32.4	33.6	
60	5	3.2		4.1	4.5	5.2	5.7	6.3	7.3	4.0	4.3	5.0	5.4	6.1	7.0	
60	15	12.8		11.9	12.8	14.7	15.9	17.5	19.8	11.3	12.1	13.8	14.8	16.2	18.3	
60	30	25.7		21.6	23.0	25.6	27.2	29.2	31.9	19.9	21.0	23.3	24.7	26.4	28.9	
90	5	1.4		2.3	2.7	3.4	4.0	4.8	6.1	1.8	2.1	2.7	3.1	3.7	4.8	
60	15	6.7		7.1	8.0	10.2	11.7	13.8	17.1	5.5	6.3	8.0	9.1	10.8	13.4	
90	30	17.0		13.0	14.6	18.0	20.2	23.1	27.1	10.2	11.4	14.2	16.0	18.4	22.1	

Table 6. Experimental and theoretical angles. Data from Ayatollahi and Aliha [10].

$\langle\varphi\rangle$	$\varphi$	$\varphi$	$\varphi$	$\varphi$
	(Erdogan-Sih) $r = 0.1$ mm	(Sih, S-factor) $r = 0.1$ mm	(Erdogan-Sih) T-stress=12.5 MPa	(Sih, S-factor) T-stress=12.5 MPa
33	30.8	30.3		
47	48.4	49.1		
60	59.1	64.5		
78	70.6	86.2	74.5	87.8

Table 5 and table 6 summarise the results taken from Refs. [9,10]. Both for cracked plates and pointed V-notches the agreement between experimental results and theoretical values is found to be satisfactory. Minimum strain energy density criterion and maximum tangential stress criterion provide a very similar assessment. The influence of the non singular stress term has been taken into account in Table 6, showing that, also in these cases, the improvement in prediction keeping into account the T-stress is low. Nevertheless the effect is interesting from a theoretical point of view. It is worth noting that Erdogan-Sih's criterion is more sensitive to the T-stress than Sih's criterion.

An example where the effect of the T-stress on fracture angle is important is reported in Table 7 referred to a simple welded lap joint [14] with a thickness  $t$ , a ligament width  $d$  and a nominal membrane stress 10 MPa. Note that the Erdogan-Sih criterion, when including the T-stress effect, gives crack initiation angles greater than those obtained by only using the singular terms of the stress fields; also in this case the Sih criterion is found to be less affected by the T-stress than the previous one.

Table 7. Example of a welded lap joint. Effect of T-stress on initial crack angle

	T-stress ( $\theta=0^\circ$ )	$\varphi$	$\varphi$	$\varphi$	$\varphi$
		Erdogan-Sih [11] without T-stress	S-factor [12] without T-stress	Erdogan-Sih with T-stress $r = 0.1$ mm	S-factor with T-stress $r = 0.1$ mm
$t=1$ mm, $d/t = 0.5$	20.0	68.1	77.2	79.7	82.3
1	19.5	62.7	66.9	78.0	75.2
2	18.0	56.1	56.0	74.0	68.3
3	17.6	55.3	54.8	73.3	67.4

## REFERENCES

1. Seweryn, A. (1994) Brittle fracture criterion for structures with sharp notches. *Eng. Fract. Mech.* **47**, 673-681.
2. Lazzarin, P., Zambardi, R. (2001) A finite-volume-energy based approach to predict the static and fatigue behaviour of components with sharp V-shaped notches. *Int. J. Fract.* **112**, 275-29.
3. Yosibash, Z., Bussiba, Ar., Gilad, I. (2004) Failure criteria for brittle elastic materials. *Int. J. Fract.* **125**, 307-333.
4. Gómez, F.J., Elices, M., Planas, J. (2005) The cohesive crack concept: application to PMMA at  $-60^{\circ}\text{C}$ . *Eng. Fract. Mech.* **72**, 1268-1285.
5. Lazzarin, P., Berto, F. (2005) Some expressions for the strain energy in a finite volume surrounding the root of blunt V-notches. *Int. J. Fract.* **135**, 161-185
6. Berto, F., Lazzarin, P., Gomez, F.J., Elices, M. (2007) Fracture assessment of U-notches under mixed mode loading: Two procedures based on the 'equivalent local mode I' concept. *Int. J. Fract.* **148**, 415-433.
7. Gómez, F.J., Elices, M., Berto, F., Lazzarin, P. (2009) Fracture of U-notched specimens under mixed mode experimental results and numerical predictions. *Eng. Fract. Mech.* **76**, 236-249.
8. Gómez, F.J., Elices, M., Berto, F. and Lazzarin, P. (2009). Fracture of V-notched specimens under mixed mode (1+2) loading in brittle materials. Submitted.
9. Chen, D.H., Ozaki, S. (2008) Investigation of failure criteria for a sharp notch, *Int. J. Fract.*, **152**, 63-74.
10. Ayatollahi, M.R., Aliha, M.R.M. (2009) Analysis of a new specimen for mixed mode fracture tests on brittle materials, *Eng. Fract. Mech.*, in press doi:10.1016/j.engfracmech.2009.02.016.
11. Erdogan, F. and Sih, G.C. (1963) On the crack extension in plates under plane loading and transverse shear, *J. Basic Eng.*, Trans ASME 85d, 519-525.
12. Sih, G.C. (1974) Strain-energy-density factor applied to mixed mode crack problems. *Int. J. Fract.* **10**, 305-321.
13. Lazzarin, P., Berto, F., Elices, M. and Gómez F.J. (2009) Brittle failures from U- and V-notches in mode I and mixed, I+II, mode. A synthesis based on the strain energy density averaged on finite size volumes, *Fatigue Fract. Engng Mater Struct*, under review.
14. Lazzarin, P., Berto, F., Radaj, D. (2009) Fatigue-relevant stress field parameters of welded lap joints: pointed slit tip versus keyhole notch. *Fatigue Fract. Engng Mater. Struct.*, under review.